ACS APPLIED POLYMER MATERIALS

pubs.acs.org/acsapm Article

Highly Hydrated Thin Films Obtained via Templating of the Polyelectrolyte Multilayer Internal Structure with Proteins

Aurélien vander Straeten* and Christine Dupont-Gillain*

Cite This: *ACS Appl. Polym. Mater.* 2020, 2, 2602−2611 Read Online

ACCESS | Metrics & More | Article Recommendations | Supporting Information

ABSTRACT: Controlling the sequence in which macromolecules interact allows creating self-assemblies that only exist because of the construction path that was followed. Because structure correlates with function, exploring paths of self-assembly holds the potential to confer various functionalities to the assembly. In this paper, lysozyme (Lyz) was used as a templating agent in the layer-by-layer (LbL) self-assembly of poly(allylamine hydrochloride) (PAH) with poly(styrenesulfonate) (PSS). To do so, Lyz was complexed with PSS, and the resulting complex was alternately adsorbed with PAH. By carrying the LbL assembly at low pH and in pure water, PAH adsorption causes the subsequent release of Lyz. The result is that even though it was used for assembly, only a very small fraction of Lyz is present in the resulting film. Using quartz crystal microbalance with dissipation monitoring mounted with a humidity module, the swelling/deswelling behavior and the composition of these polyelectrolyte multilayers (PEMs) were investigated. It appears that such PEMs obtained via a complex adsorption sequence are much thicker and trapped in a nonequilibrium state. Their dehydration is irreversible as it causes their collapse into denser PEMs. After dehydration, the PEMs share a common composition with the ones constructed without the use of Lyz as a templating agent. Fitting the Flory−Huggins equation to the data suggests that both PEM types separate into a polymer-rich phase and a water-rich phase when exposed to increasing water vapor pressure. Nevertheless, the presence of a swelling hysteresis in the PEMs templated with Lyz suggests that they possess a different internal structure or that trace amounts of Lyz affect the polymer relaxation kinetics. The use of proteins as templating elements thus allows to construct PEMs that are thick, highly hydrated, and gel-like at the nanoscale level rather than thin dense PE blends, which is topical for biomedical applications.

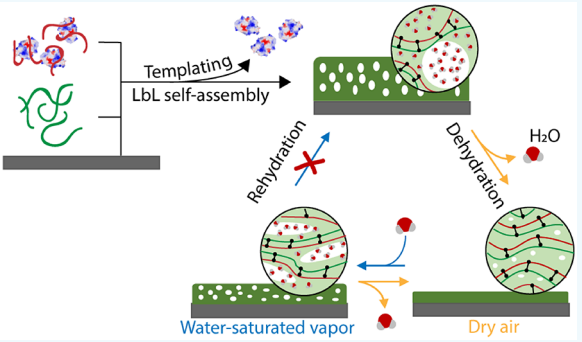

KEYWORDS: *self-assembly, quartz-crystal microbalance, humidity, polyelectrolyte multilayer, thin film, hydration*

Downloaded via UNIV CATHOLIQUE DE LOUVAIN on June 9, 2021 at 08:41:47 (UTC).
See https://pubs.acs.org/sharingguidelines for options on how to legitimately share published articles.

INTRODUCTION

Layer-by-layer (LbL) assembly is a widely used method for engineering materials and coatings.[1,2] It consists in the alternate adsorption of species (macromolecules, particles, etc.) which results in a multilayered self-assembly. The hierarchical nanostructures that are obtained are out-of-equilibrium, which means that they are not at their lowest energy state.[3] This is achieved because the path followed for buildup dictates the final state that is reached. Polyelectrolytes (PE) are among the most used materials for LbL assembly. Interestingly, the layered nanoarchitecture of the PE multilayers (PEMs) that are obtained displays functional properties such as a high sensitivity to ambient moisture, the ability to strongly interact with light, or to release trapped molecules via a stimulus.[4−6] These properties are attributed to the layered structure of PEMs and therefore emerge from the path that has been followed to self-assemble the macromolecules.

The response to ambient moisture that originates from the nanolayered structure of PEMs has been under investigation for the two past decades. Indeed, PEMs were shown to exhibit a measurable swelling and plasticization upon exposure to an increasing water vapor pressure.[7,8] This swelling/deswelling behavior allowed to study the PEMs internal structure, but it also makes them particularly well suited for humidity-sensing devices.[4,5,7] In particular, PEMs constructed via the alternate adsorption of poly(allylamine hydrochloride) (PAH) and poly(styrenesulfonate) (PSS) have been intensively investigated. Lösche et al. demonstrated that water occupies 40% of the volume in [PAH−PSS] PEMs when the air is saturated with water vapor.[9] The number of water molecules per PE chain can be notably high in these conditions. For instance, it has been reported for [PAH−PSS] that eight water molecules are present per anion−cation ionic pair.[8] Other systems such as PSS/

Received: March 9, 2020
Accepted: May 26, 2020
Published: May 26, 2020

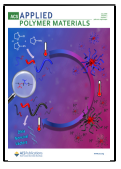

ACS Publications © 2020 American Chemical Society

https://dx.doi.org/10.1021/acsapm.0c00243
ACS Appl. Polym. Mater. 2020, 2, 2602−2611

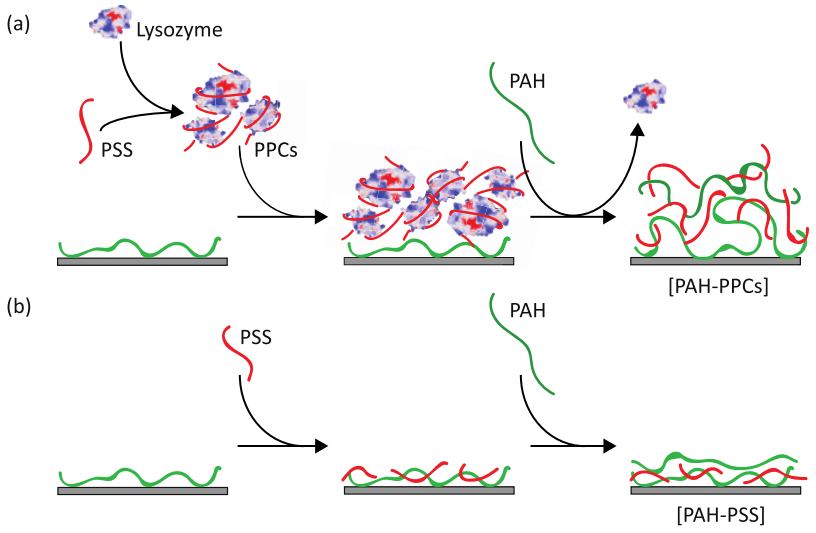

Figure 1. (a) Schematic of the formation of PPCs and subsequent LbL assembly with PAH. When constructed at low pH and low salt concentration, this results in the release of Lyz molecules upon assembly. (b) Schematic of the classical alternate adsorption of PAH and PSS and the resulting PEM.

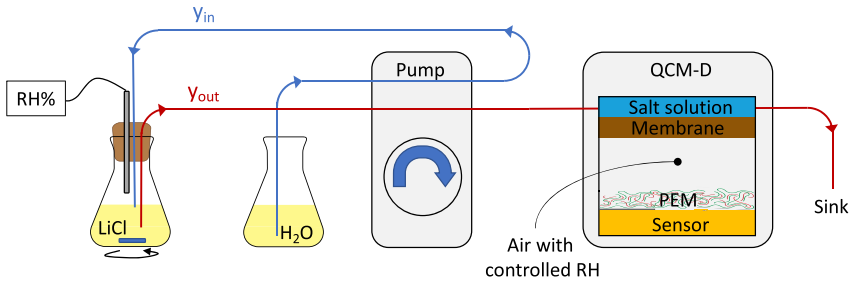

Figure 2. Schematic of the experimental setup used to vary the RH of the air in contact with PEMs, in a QCM-D cell equipped with a humidity module. The QCM-D sensor is in direct contact with a small air volume, itself separated by a membrane from a circulating solution. A saturated LiCl solution is continuously diluted with water (y_{in}) and pumped through the QCM-D humidity module (y_{out}). The decrease in LiCl concentration in the flowing solution causes an increase in RH in the QCM-D cell. The water and LiCl vessels can be inverted to obtain a decrease in RH. In the latter case, the water solution is mixed with a concentrated LiCl solution.

poly(diallyldimethylammonium chloride) (PDADMAC) were found to have six water molecules per complex.[10] With respect to the swelling kinetics, Kügler et al. reported that hours were needed to reach equilibrium in [PAH−PSS] PEMs.[11] In contrast, Wong et al. reported that only a few minutes was needed for the same PEMs.[12] This difference might be due to the different salt concentration used to construct the PEMs. The swelling behavior has been shown to be split into distinct modes. When going from low to high relative humidity (RH), a swelling transition occurs from a state where water and PEs are homogeneously distributed to a state where water and PEs are phase-separated. For instance, this transition was observed at a RH of 60% and a volume increase of 20% for PEMs made with [PSS-poly(diallyldimethylammonium chloride)-*N*-methyl-*N*-vinylacetamide].[13] By measuring the thickness as a function of RH, Secrist et al. demonstrated a swelling/deswelling hysteresis in PEMs made of [PAH-poly(acrylic acid) (PAA)].[4] Moreover, they have shown for [PAH−PAA] PEMs that depending on the building conditions, different degrees of hysteresis could be obtained. It was suggested that different water transport mechanisms and internal molecular restructuration kinetics were at play upon swelling and deswelling, which caused hysteresis in the swelling behavior.[4] In all reported cases, the hydrated and dehydrated states were completely reversible, and the PEMs response to ambient moisture was highly dependent on both the PE nature and assembly conditions.[13−15]

It was recently shown that PEMs constructed via more complex adsorption sequences may possess particular hydration properties.[16,17] Especially, it has been found that a protein can be used as a templating agent to create highly hydrated PEMs. These PEMs are obtained by first complexing the protein with a PE in solution and then alternating the adsorption of the so-called protein−PE complex (PPC) with an oppositely charged PE. This procedure was demonstrated for lysozyme (Lyz) complexed with low molar mass PSS and assembled with PAH. When these multilayers were constructed at pH 3, without any other electrolyte than the ones used to adjust pH and the counterions of the PEs, i.e., in conditions in which PAH is fully ionized and long-range electrostatic forces are prevalent, PAH was shown to substitute Lyz from the PPCs upon assembly. As represented in Figure 1a, this results in a PEM that is almost only made of PAH and PSS, and has a very high water content. With PPCs, it is thus possible to obtain PEMs that are made with the same constituents as in $[PAH−PSS]_5$ PEMs (constructed as shown in Figure 1b), but with a hydration level that is completely different. Therefore, their internal structure must also be very different.

Because structure correlates with function, designing new structures could pave the way to new functionalities. For instance, the comparison of PEMs grown in different pH or salt conditions, i.e., PEMs with different structures, has been one of the major drivers of innovation in the field of LbL assembly (the

https://dx.doi.org/10.1021/acsapm.0c00243
ACS Appl. Polym. Mater. 2020, 2, 2602−2611

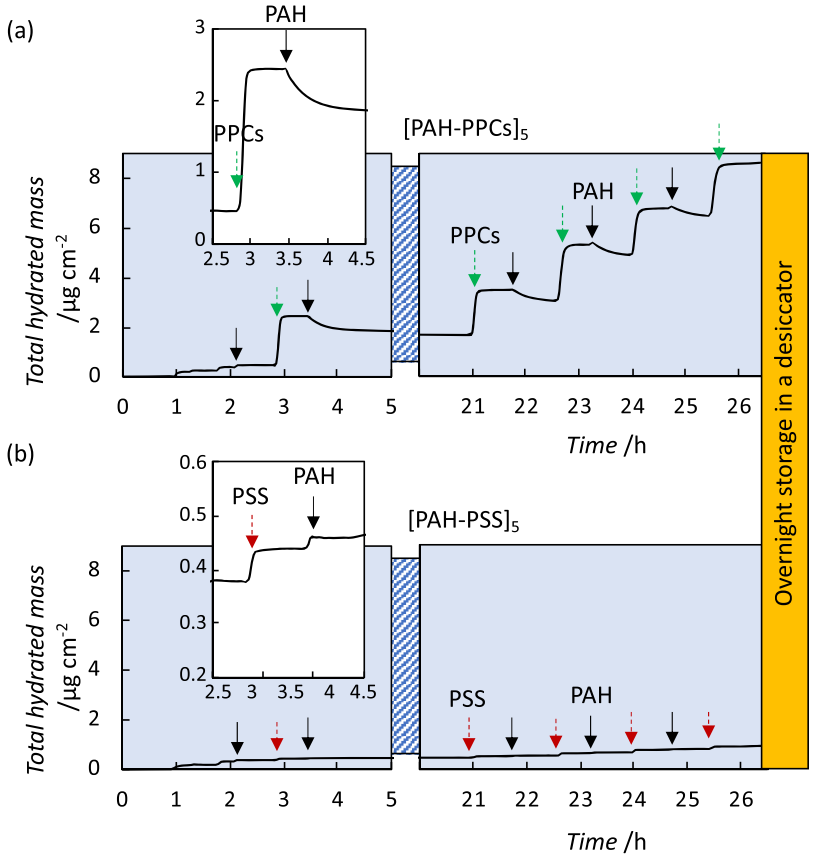

Figure 3. (a) $[PAH-PPCs]_5$ and (b) $[PAH-PSS]_5$ are constructed in the QCM-D flow module. PAH, PPCs, and PSS adsorption steps are indicated by a black solid arrow, a green dashed arrow, and a red dashed arrow, respectively. PPCs are obtained by mixing PSS with Lyz prior to the adsorption. In all cases, the first 2 h corresponds to the deposition of a $[PAH-PSS_h]_2$ anchoring layer. For clarity, these two bilayers are not indicated with arrows. The dashed box corresponds to an overnight storage in water at pH 3. Multilayers were washed for 20 min with water at pH 3 between each adsorption step. After the construction of five bilayers, PEMs are dehydrated via an overnight storage in a desiccator followed by exposure to a nitrogen flux (yellow box). Insets: enlarged graph portions showing the deposition of a bilayer with more details.

very first papers published on the subject studied the effect of salt on PEMs formation).[18] It is thus essential to investigate how the use of PPCs affects the properties of the resulting PEMs. Especially, the focus can be set on the ability to swell/deswell as a function of water vapor pressure, as this is the main functionality that arises from the hierarchical structure created through the LbL assembly of simple PEs.

This paper aims at investigating the hydration properties of classical PEMs vs PEMs that were constructed with a templating agent. In particular, water uptake/release as a function of relative humidity and PEM composition could shed light onto the internal structure and the PE chain mobility. PEMs were thus constructed on a quartz crystal microbalance with dissipation monitoring (QCM-D) sensor in the regular flow module by alternately adsorbing five layers of PAH with PSS ([PAH−PSS]), or PAH with Lyz/PSS-based PPCs ([PAH−PPCs]), at pH 3 in water. A convenient way to measure water sorption/desorption in PEMs is the use of QCM-D mounted with a so-called humidity module. In this module, the coated QCM-D sensor is separated from a solution by a membrane that is only permeable to water (see Figure 2 for a schematic of the QCM-D humidity module).[19] Usually, different salt solutions are pumped through the humidity module to obtain different (discrete) RH values in the air chamber that is in contact with the sensor. In this report, a saturated LiCl solution is pumped through the humidity module, which gives a RH of 11% in the air above the sensor. In the meantime, the LiCl solution is continuously diluted by water that is pumped-in at constant volumetric rate. Depending on the LiCl molality in the flowing solution, different water activities are obtained (a_w), resulting in a gradient of RH of the air in contact with the sensor (see Figure 2 for the experimental setup). This allows RH to be controlled from 11% to 99.9%, i.e., 99.9% being when LiCl is highly diluted. The water and LiCl solution vessels can be inverted to obtain a decrease in RH. In the latter case, the water solution is mixed with a concentrated LiCl solution. The mass variation of PEM upon RH variation can be measured to construct water sorption/desorption isotherms.

MATERIALS AND METHODS

PEMs Formation. $[PAH-PSS]_5$ and $[PAH-PPCs]_5$ were constructed at pH 3 in water by using our previously reported method.[16] Commercially available 4.95 MHz AT-cut gold-coated quartz sensors (purchased from Q-Sense, Stockholm, Sweden) were used. These sensors were washed with H_2O_2/H_2SO_4 1:3 (v:v) solution, successively rinsed with water and ethanol, and then exposed to UV-ozone prior to measurement. Layer growth on gold-coated sensors was monitored by using a QCM-D system (Q-Sense E4 system, Q-Sense, Stockholm, Sweden). The solution flow rate and temperature were respectively set at 20 μL min^{-1} and 20 °C. For all experiments, two bilayers of PAH (M_w = 17500 g mol^{-1}, chloride salt form, Sigma-Aldrich, Steinheim, Germany) alternately adsorbed with high molar mass PSS (PSS_h, M_w = 70000 g mol^{-1}, sodium salt form, Sigma-Aldrich, Steinheim, Germany) were constructed from PAH and PSS_h solutions (0.5 g L^{-1} for both PEs; for PAH, the ionic strength (I) is of 3.67 mM

https://dx.doi.org/10.1021/acsapm.0c00243
ACS Appl. Polym. Mater. 2020, 2, 2602−2611

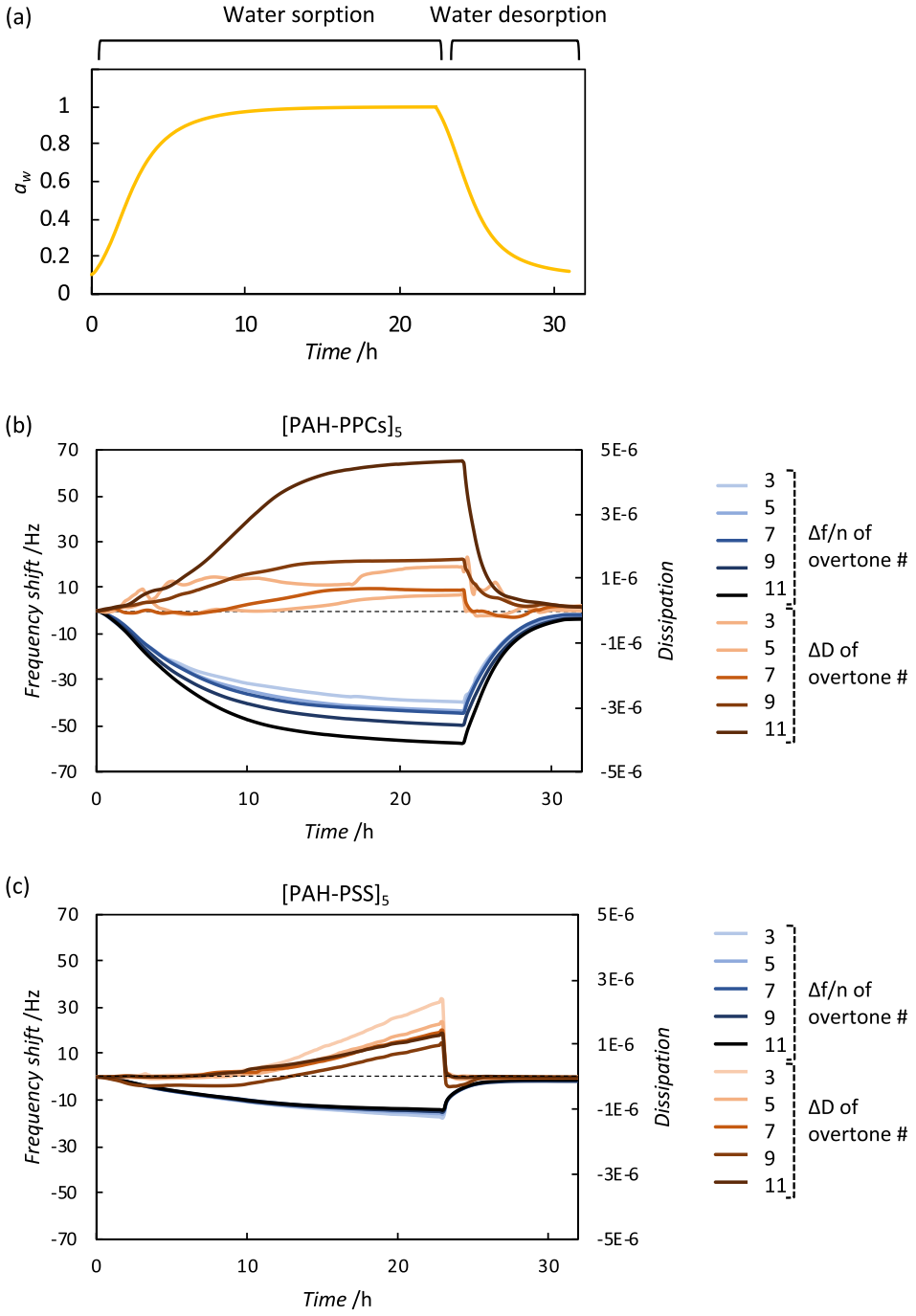

Figure 4. (a) Computed profile of a_w variation as a function of time. Normalized frequency shift ($\Delta f/n$) and dissipation shift (ΔD) measured for sensors coated with (b) $[PAH{-}PPCs]_5$ or (c) $[PAH{-}PSS]_5$ as a_w varies according to the profile shown in (a).

and monomer concentration ≃5.36 mM, and for PSS $I \simeq 2.21$ mM and monomer concentration ≃2.42 mM) to form a standard anchoring layer. Because these two bilayers were constructed for all experiments, they will not be systematically mentioned when referring to the different assemblies created. Then, two different multilayers were built on this anchoring layer: PAH assembled with PSS or PAH assembled with PPCs. The following solutions were used: PAH (0.5 g L^{-1}, same as above), PSS (0.030 g L^{-1}, $I \simeq 1.07$ mM, monomer concentration ≃0.14 mM, M_w = 7540 g mol^{-1}, M_w/M_n = 1.08, Scientific Polymer, Ontario, NY), and PPCs. PPCs were prepared by mixing two volumes of PSS (0.104 g L^{-1}, $I \simeq 1.25$ mM, monomer concentration ≃0.49 mM) solution with five volumes of a Lyz (0.178 g L^{-1}, Sigma-Aldrich, Steinheim, Germany, IEP = 11.35).[16] All solutions were prepared in ultrapure water, and the pH was adjusted to 3 with HCl. Each adsorption step lasted 40 min and was followed by rinsing for 20 min with water at pH 3. The changes in frequency and dissipation were recorded. The mass adsorbed on QCM crystals was assessed using the Sauerbrey equation for the seventh overtone: $\Delta m = -C\Delta f_7 \cdot 7^{-1}$, where Δm is the shift of adsorbed mass per surface area (μg cm^{-2}), Δf_7 the frequency shift measured for the seventh overtone (Hz), and C a constant equal to 17.7 ng cm^{-2} Hz^{-1} for a 5 MHz crystal.[20] Results of the PEM construction are presented in Figure 3. Because it takes more than 1 day to build such systems, the films were rinsed with water at pH 3 and left for a night in the QCM-D flow module after the construction of a $[PAH{-}PSS_h]_2$ anchoring layer followed by the first bilayer of each system. This is represented by the blue dashed box in Figure 3 (between 5 and 20 h of construction). After construction, the coated sensors were stored one night in a desiccator before being mounted in the humidity

https://dx.doi.org/10.1021/acsapm.0c00243
ACS Appl. Polym. Mater. 2020, 2, 2602−2611

module of the QCM-D. This storage step is represented by the yellow box in Figure 3.

Water Sorption/Desorption Isotherms Measurement. The method proposed by Graf and Kocherbitov was used to continuously change the RH of the air in contact with the coated sensor between 11% and 99.9%.[19] To do so, the setup presented in Figure 2 was constructed. A saturated LiCl solution was prepared by dissolving 45 g of dry LiCl in 50 mL of water. Solutions were left under stirring 3 days for stabilization and then filtered first on a 5 μm cellulose filter and then on a 0.45 μm poly(ether sulfone) filter. 25 mL of the obtained saturated LiCl solution was added to a dry Erlenmeyer with a RH probe (Novasina ms1, Defensor, Lachen, Switzerland). The setup was closed hermetically and left to stabilize with a magnetic stirrer. After a few minutes, the air in the setup reached around 11% of RH. In the meantime, tubes going from the stock of water to the LiCl solution were filled with water while those going from the LiCl stock solution to the QCM-D humidity module were filled with dry N_2. The temperature of the QCM-D humidity chamber was set at 20 °C. The experiment was started by applying a flow of 0.1 $cm^3\ s^{-1}$ in both the water-to-LiCl and LiCl-to-QCM-D humidity module tubing. In this way, the LiCl solution was pumped through the QCM-D humidity module while being diluted by water at the same volumetric rate. In the meantime, the crystal resonant frequencies were acquired, and the QCM-D started to record the frequency ($\Delta f/n$) and dissipation (ΔD) shifts due to water sorption/desorption from PEMs previously deposited on the sensor as described above. Overtones ranging from the 3rd to the 11th were recorded, since overtone splicing indicates variation in the viscoelastic properties of the film. The mass variation (Δm_w) due to the water sorption/desorption was estimated via the Sauerbrey equation for the seventh overtone (see the Results and Discussion section for details). After 22.5 h, the Erlenmeyer that initially contained the saturated LiCl solution contained highly diluted LiCl, i.e., a_w = 0.999999 (which will be referred to in the following as a_w = 0.999 for clarity). At this point, the setup was inverted, and this almost pure water was mixed with a LiCl-saturated solution. After 8 h, the Erlenmeyer contained again 25 mL of a LiCl solution that is close to saturation, and consequently a gas phase with RH = 11% was in contact with the sensor.

To construct water sorption/desorption isotherms, it is critical to access the RH of the air in contact with the PEMs, i.e., directly in the humidity chamber. RH is given by a_w, which depends on LiCl molality in the flowing solution. To determine the RH of the air in contact with the sensor, the LiCl molality variation was computed as a function of time. To do so, the LiCl and water mass transfer equations were solved (see the Supporting Information section S1 for details) according to the method proposed by Graf and Kocherbitov.[19] Then, a_w as a function of LiCl molality was computed thanks to a 6-order interpolation of data reported in the literature.[19,21]

Results of the calculated a_w values are presented in Figure 4a. These values are in good agreement with the literature.[19] Moreover, the RH measured in the Erlenmeyer that initially contained LiCl is consistent with the computed a_w variation (see Figure S1). To further confirm the accuracy of the modeling, both the initial and final water and LiCl masses were measured and compared to the modeling. This was achieved by weighting solutions and evaporating their content at 150 °C. The mass difference allows to estimate the evaporated water mass, and the remaining mass is attributed to LiCl. Results are presented in Figure S1 and show a perfect match between the modeling and the measurements. Finally, the absence of uncontrolled water condensation on an uncoated gold sensor was verified. To do so, a_w was increased from 0.110 to 0.999, and the mass variation of the uncoated sensor was recorded. Results are presented in Figure S2 and confirm the absence of any measurable water sorption on an uncoated sensor.

RESULTS AND DISCUSSION

PEM Construction. Results of the construction of $[PAH-PPCs]_5$ and $[PAH-PSS]_5$ are respectively presented in Figures 3a and 3b. In both cases, a stepwise mass increase of the PEM is observed, which confirms that the LbL assemblies grow. For $[PAH-PPCs]_5$, a "sawtooth" profile is observed, and the total PEM hydrated mass decreases upon each PAH adsorption step but strongly increases after each PPCs deposition step. The net result is that the multilayer mass increases stepwise. After the deposition of five bilayers, the $[PAH-PPCs]_5$ multilayer reached a total hydrated mass of 8 $\mu g\ cm^{-2}$, while $[PAH-PSS]_5$ reached only 1 $\mu g\ cm^{-2}$. When PPCs are adsorbed, the film reaches equilibrium after only a few minutes, while the time needed to reach equilibrium after PAH adsorption is much longer (see the inset in Figure 3a). This suggests that the film undergoes slow molecular rearrangement after PAH addition. The multilayers were constructed in conditions in which PAH is fully ionized, i.e., at pH 3. As a consequence, when the highly positively charged PAH is adsorbed onto PPCs, it substitutes Lyz from the latter, which releases Lyz from the multilayer. The protein amount was quantified by using a bicinchoninic acid assay (BCA) using the protocol reported earlier.[16] It appears that only 100 ng cm^{-2} of Lyz is detected in $[PAH-PPCs]_5$ which represents only 1.4 ± 0.2% of the initial total hydrated PEM mass, therefore confirming Lyz release from the multilayer. This result is also consistent with our recent demonstration that when the same multilayer is constructed at pH 7.5, the PAH lower ionization degree impedes Lyz substitution from the PPCs. When pH is decreased to a value of 5, the increased PAH ionization degree causes Lyz to be released from the multilayer.[22] Note that the multilayers grow at a linear rate thanks to the $[PAH-PSS_h]$ anchoring layer that screens the effect of the underlying surface. When PPCs were adsorbed, the multilayer mass increased by an average of 1.94 $\mu g\ cm^{-2}$ at each adsorption step, while when PSS was adsorbed the average mass increase was of 0.08 $\mu g\ cm^{-2}$ at each adsorption step (see insets in Figure 3a,b). After the construction of $[PAH-PPCs]_5$ and $[PAH-PSS]_5$ in the flow module of the QCM-D, they were stored one night in a desiccator (represented as the yellow box in Figure 3).

PEM Hydration/Dehydration Cycles. After the PEM construction and the overnight storage in a desiccator, the coated sensors were mounted in the humidity module. The a_w of the solution flowing in the QCM-D humidity module was first brought to 0.110—the air in contact with the PEMs thus has a RH of 11%—and the resonant frequencies were determined. The $[PAH-PPCs]_5$ and $[PAH-PSS]_5$ PEMs were then exposed to a cycle of hydration and dehydration. To do so, a_w was increased from 0.110 to 0.999 and then brought back from 0.999 to 0.110 (see Figure 4a for the profile of a_w variation as a function of time). During the whole cycle of a_w variation, the $\Delta f/n$ and ΔD of the overtones 3−11 were recorded. Results are presented in Figure 4b for $[PAH-PPCs]_5$ and in Figure 4c for $[PAH-PSS]_5$. It appears that as a_w increases, $\Delta f/n$ decreases, and ΔD increases for both PEMs. This suggests that both PEMs take up water and hence that their viscoelasticity increases. This is consistent with the plasticization reported for similar systems at high RH.[13] When a_w is brought back from 0.999 to 0.110, $\Delta f/n$ increases and ΔD decreases, which suggests that water is released from the PEMs and that they become more rigid again.

To convert $\Delta f/n$ into a mass of water absorbed by the PEM, several mathematical models exist. The Sauerbrey equation is the simplest. It assumes laterally homogeneous thin film that are as rigid as the quartz sensor. Both $[PAH-PPCs]_5$ and $[PAH-PSS]_5$ are sufficiently close to these conditions (see the Supporting Information section S3 for details). Water sorption/desorption (Δm_w) was thus computed as a function of time by using the Sauerbrey equation. Because a_w variation with time is not linear, interpretation of Δm_w variation is not

https://dx.doi.org/10.1021/acsapm.0c00243
ACS Appl. Polym. Mater. 2020, 2, 2602−2611

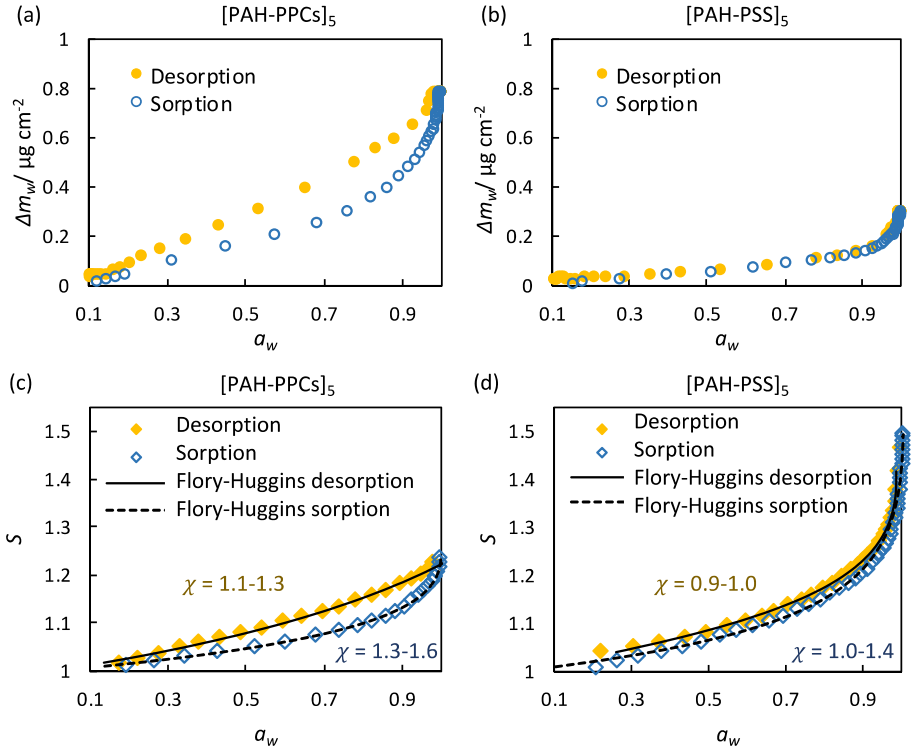

Figure 5. Water sorption/desorption isotherms Δm_w as a function of a_w for (a) $[PAH-PPCs]_5$ and (b) $[PAH-PSS]_5$. Swelling parameter S as a function of a_w and fitting of the Flory–Huggins equation with variable χ (black lines) for (c) $[PAH-PPCs]_5$ and (d) $[PAH-PSS]_5$.

straightforward. To clearly identify PEM swelling/deswelling transitions, which are key characteristics, Δm_w was expressed as a function of a_w. Results are presented in Figure 5a,b. Only one full data set for each PEM is shown in Figure 5, but the experiment was repeated three times (see Figure S3 for all replicates). Both the initial and final Δm_w values of all replicates will be used later in this paper to obtain statistics on the PEM composition. When a_w increases from 0.110 to 0.8 for $[PAH-PPCs]_5$ and from 0.110 to 0.9 for $[PAH-PSS]_5$, both PEMs take up water at a relatively constant rate, i.e., with a linear increase of Δm_w as a function of a_w. Above these respective a_w values, the water sorption rate increases exponentially. The water sorption displayed in Figure 5a,b suggests that as a_w increases, the amount of solvent that can be absorbed increases, i.e., the solubility coefficient increases with the solvent vapor pressure. Such a sorption mode is well described by the Flory–Huggins theory, which provides a direct relationship between a_w and the polymer swelling, based on the polymer–solvent interaction parameter χ.[23] χ is a dimensionless quantity characterizing the difference in interaction energy of a solvent molecule immersed in pure polymer compared with one in pure solvent.[4,13]

In a view to interpret our data by using the Flory–Huggins theory, the Δm_w values were converted into thickness variation and the swelling parameter S was computed ($S = d_s + d_0^{-1}$, where d_s is the thickness at a given a_w while d_0 is thickness when a_w = 0.110; see the Supporting Information section S4 for details). Then, the Flory–Huggins equation was fitted to our data sets (see Figure S4), and the polymer–solvent interaction parameter χ was computed.[13] The best fitting of water sorption/desorption in $[PAH-PPCs]_5$ PEM was obtained for χ = 1.4 and 1.2 respectively for water sorption and desorption (see Figure S4a). For $[PAH-PSS]_5$, a χ value of 1.1 for both water sorption and desorption (see Figure S4b) was obtained. The latter result is consistent with the reported χ value of 0.9 for the $[PAH-PSS]$ system constructed at neutral pH.[11] According to the Flory–Huggins theory, a χ value higher than 0.5 means that the polymer–solvent interaction is strongly repulsive and that, as a consequence, the polymer phase separates from the solvent when a_w increases. Our results thus strongly suggest that the water sorption is accompanied by a phase separation, which leads to PE-rich phases separated by domains of pure water. This hypothesis is supported by the strong increase in softness observed for both PEMs at high RH (as indicated by the increase of ΔD in Figure 4b,c). Importantly, a deviation of the initial Flory–Huggins theory was proposed in the literature, suggesting that χ can decrease with increasing a_w in PE-based systems, i.e., the affinity of water for PE increases with a_w.[4,24] The data were thus fitted again, but this time χ was allowed to vary quadratically with S (see the Supporting Information section S4 for details). Results of the fitting as a function of a_w and for variable χ values are presented in Figure 5c,d. The χ value as a function of a_w for both PEMs is presented in Figure S5. While the fitting appears to be much better than with constant χ, the obtained χ values are close to the previous fitting and do not decrease significantly at high a_w, which suggests that phase separation is maintained, even at high RH. PEMs were constructed at low pH, which means that both PAH and PSS are fully ionized. As a consequence, the ion pairing is maximal. Yet, PAH–PSS ion pairing is among the strongest possible interaction for PE–PE pairs, which could explain why water does not penetrate the polymer-rich phase, even at very high RH.[25]

Interestingly, water desorption differs from water sorption in $[PAH-PPCs]_5$ while there is no such hysteresis in $[PAH-PSS]_5$ (Figure S3 shows the replicates all displaying the same behavior). When compared to other experimental setups previously used to measure water sorption/desorption in PEMs, the one used here allows the water uptake/release to be measured *in situ* and continuously. While this system reveals

https://dx.doi.org/10.1021/acsapm.0c00243
ACS Appl. Polym. Mater. 2020, 2, 2602–2611

much better the dynamic properties of PEMs upon varying water vapor pressure, the PEMs might not be at equilibrium. Especially, when comparing sorption and desorption, the a_w variation rate differs when RH is increased vs decreased (see Figure 4a). As a consequence, the hysteresis observed $[PAH-PPCs]_5$ might be partially due to a different rate of a_w variation. Yet, when comparing $[PAH-PPCs]_5$ to $[PAH-PSS]_5$, we applied the same a_w variation rate. Therefore, while the hysteresis might be affected by hydration/dehydration kinetics, it still indicates that both PEMs respond differently to ambient moisture. Swelling/deswelling hysteresis were sometimes observed depending on the conditions and PEs that are used to construct PEMs.[4] For instance, when [PAH−PAA] multilayers are constructed at intermediate pH values, PE chain mobility is high because both PEs are not fully ionized. This is believed to cause the swelling/deswelling hysteresis. In contrast, [PAH−PAA] PEMs constructed at low pH, i.e., with fully ionized PAH, display a very small swelling/deswelling hysteresis due to lower PE chain mobility.[4] This is perfectly consistent with the absence of water sorption/desorption hysteresis observed for $[PAH-PSS]_5$. Indeed, the latter PEM was constructed at pH 3, with both PEs thus fully ionized, and chain mobility is at its lowest. For $[PAH-PPCs]_5$, the sorption/desorption hysteresis suggests a high PE chain mobility. This latter feature is surprising as this PEM was also constructed at pH 3 and contains mainly PAH and PSS. The only difference between these systems is that a protein was used as a templating agent when PPCs were used and that trace amounts of Lyz are present in the latter.

A comprehensive analysis of PEMs composition was thus carried out. To do so, resonant frequencies of the naked sensors (before multilayer construction) were determined in the humidity chamber (a_w set at 0.110). Then, the PEMs were constructed in the flow module of the QCM-D. The coated sensors were then mounted again in the humidity chamber, a_w was set at 0.110, and the resonant frequencies were determined again (see Figure S6). The shift between the resonant frequency before and after multilayer construction is thus due to the multilayer mass under a_w = 0.110, and it was used to compute the PEM dry mass. Results of the PEMs dry mass are presented in Figure 6 as the plain orange bar. In the same chart, the PEM mass after construction in water (in the flow module, before any dehydration step) is presented as the dashed blue bar, and the water sorption/desorption measured via the experiments that are presented in Figures 4 and 5 is shown as the plain blue bars. The protein amount was quantified using a BCA assay using the protocol reported previously.[16] It appears that only 100 ng cm^{-2} of protein can be detected in $[PAH-PPCs]_5$, which represents only 1.4 ± 0.2% of the initial total hydrated PEM mass and 2.6 ± 1.4% of the PEM dry mass (see Figure 6a). Note that the total rehydrated mass is represented as the sum of the dry mass and the water uptake in water-saturated air. Results show that $[PAH-PPCs]_5$ fails to recover its initial total mass in water vapor-saturated air after undergoing dehydration in the desiccator. Indeed, the PEM recovers only 68 ± 12% of its mass, i.e., 4.93 ± 0.49 μg cm^{-2} (protein mass + dry mass + water mass), after full rehydration in the humidity chamber (errors are propagated). On the contrary, $[PAH-PSS]_5$ fully recovers its initial total mass under high RH as shown in Figure 6b. The initial hydrated mass was measured in water while the water sorption is measured in water-saturated air. $[PAH-PPCs]_5$ thus cannot recover its hydration level under high RH. The latter is different from an aqueous solution even if a_w = 1 in both the water-saturated air and aqueous solution. We tried to measure

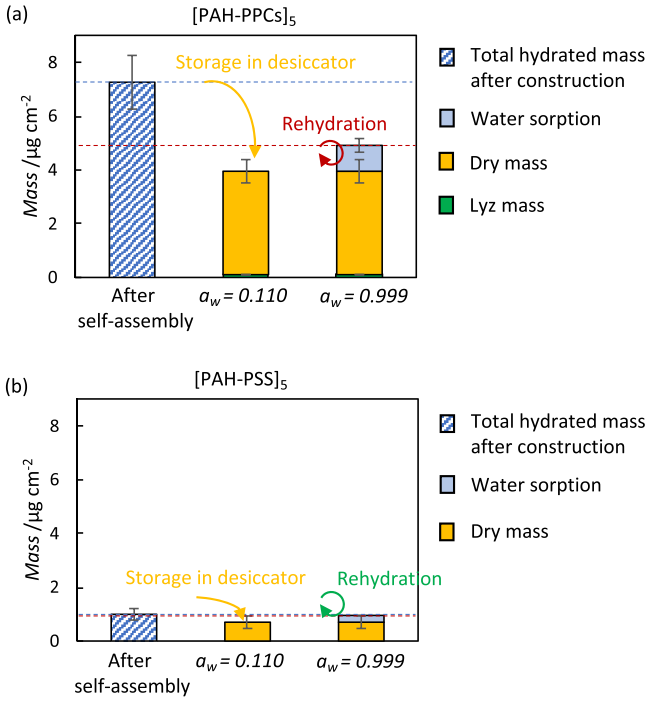

Figure 6. Composition of (a) $[PAH-PPCs]_5$ and (b) $[PAH-PSS]_5$ PEMs. The dashed blues bars show the PEM hydrated mass after self-assembly in the flow module of the QCM-D (no dehydration). The green bars show the Lyz amount. The orange bars show the dry mass of the PEM measured in the humidity chamber (a_w = 0.110). The plain blue bars show the water sorption (measured in the humidity chamber; number of replicates ≥3).

the rehydration in water (in the QCM-D flow module rather than in water vapor-saturated air), but we failed to reproduce accurately the measurement and obtained unstable resonant frequencies. The PSS:Lyz weight ratio is 1:2 (w:w) in the PPCs solution that is adsorbed onto the PAH layer, while the dry PEM:Lyz weight ratio is 1:0.026, i.e., 0.007 nmol of Lyz per cm^2. Lyz is thus not an additive but a true templating agent that is removed from the PEM as the latter grows.

Results shown in Figure 6 suggest that $[PAH-PPCs]_5$ irreversibly loses part of its water content after the first dehydration step, while $[PAH-PSS]_5$ fully recovers its hydration level. The number of water molecule per PSS−PAH ionic pair (protonated amine pairing with sulfonate) that can be lost upon dehydration, i.e., loosely bound water molecules, was computed. Assuming that each PEM contains an equal number of positively and negatively charged functions and that all ionic pairs are formed, i.e., counterions are released from the PEM, the number of moles of sulfonate−amine ionic pairs ($p_\pm$) in the PEM can be found according to

$$p_{+/-} = m_{dry}/(Mr_{PSS} + Mr_{PAH})$$

where m_{dry} is the PEM dry mass and Mr_{PSS} and Mr_{PAH} are the molar masses of the repeating units of PSS and PAH. Because the self-assembly was performed at pH 3, all amines and sulfonates are respectively positively and negatively charged. With this equation, the PEM is approximated to a collection of ionic pairs ($p_\pm$) formed between the repeating units of PAH and PSS. Once $p_\pm$ was known, the number of loosely bound water molecules was computed based on the difference between the dry mass and the hydrated mass. The hydrated mass after self-assembly was considered to compute the number of loosely

https://dx.doi.org/10.1021/acsapm.0c00243
ACS Appl. Polym. Mater. 2020, 2, 2602−2611

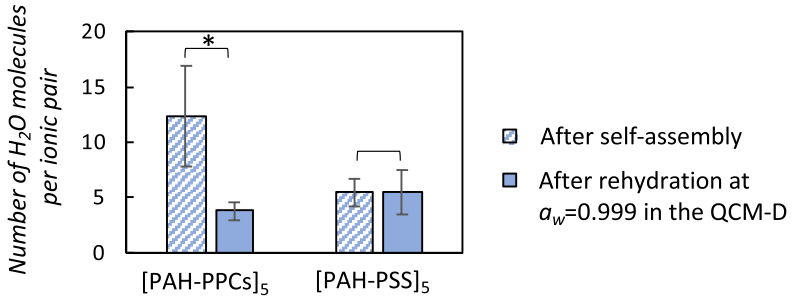

Figure 7. Number of loosely bound water molecule per PAH−PSS ionic pair. Data connected with a star are statistically different (number of replicates ≥3, α = 5%).

bound water molecules after self-assembly, while the hydrated mass after overnight storage in the desiccator and subsequent rehydration in the QCM-D humidity chamber was considered for the number of loosely bound water molecules after rehydration. Finally, results were expressed as the number of loosely bound water molecules per $p_{\pm}$. These are presented in Figure 7 for both PEMs. $p_{\pm}$ is likely overestimated since m_{dry} represents not only the mass of PE but also the one of water molecules that did not evaporate in the low-RH environment and the counterions not released from the PEM. Because of the loopy nature of PSS due to the presence of Lyz as a templating agent, $p_{\pm}$ is also likely to be overestimated after self-assembly. After dehydration, the fitting of our data with the Flory−Huggins equation shows a phase separation when the PEMs are rehydrated. Therefore, it can be concluded that the ionic pairs are all formed and that a dense polymer phase separates from the water phase. If all pairs were not formed, a homogeneous phase would be obtained given the highly hydrophilic nature of both PAH and PSS. The number of loosely bound water molecules per $p_{\pm}$ found in the latter case is thus a good estimate, while the one found after self-assembly is likely underestimated. Results show that the number of loosely bound water molecule per $p_{\pm}$ decreases after dehydration for [PAH−PPCs]$_5$, i.e., from 12 to 4, while it stays constant for [PAH−PSS]$_5$ with around 5 water molecules per $p_{\pm}$. The result obtained for [PAH−PSS]$_5$ is in the range of the reported 8 water molecules per $p_{\pm}$ for a [PAH−PSS] PEM constructed in acidic conditions.[8,9]

When a [PAH−PPCs]$_5$ multilayer is constructed, it has a hydrated mass that is drastically different from [PAH−PSS]$_5$, i.e., it is 8-fold heavier (see Figures 3 and 6). LbL films were already classified as "nanogels" by Chacko et al. due to their high water content and the use of soluble polymers.[26] [PAH−PPCs]$_5$ films definitely match this definition given their very high volume fraction of water (see Figure 6). Importantly, this feature is in principle not encountered for PEMs constructed in conditions in which Debye screening is at its lowest and all PEs used are at their highest ionization degree. Indeed, thin and compact LbL films, such as the [PAH−PSS]$_5$ PEM obtained in this study, are expected in such conditions due to high intramolecular electrostatic repulsion. The use of PPCs to construct PEMs is thus relevant for applications that are limited to specific conditions of the solution, i.e., the absence of salt and buffer or the use of highly ionized macromolecules, but that aim to obtain highly hydrated films. For instance, cells grown on these multilayers could have drastically different behavior since hydration and charge influence their differentiation and migration.[27]

Both PEMs were constructed under the same conditions (pH 3, low I) and resulted in films that are made with similar constituents (water, PAH, and PSS; only 100 ng cm^{-2} of Lyz are detected in [PAH−PPCs]$_5$). Interestingly, it means that the content of the LbL films does not reflect the stoichiometry of constituents that were used to grow it. PEMs were indeed already shown to display different internal stoichiometry depending on the building conditions.[28] Even if this is sensible, especially for out-of-equilibrium systems, it stresses the need for a complete analysis of any PEM when constructed. Indeed, the constituents of a LbL system are frequently assumed based solely on the observation of a stepwise mass increase or a charge inversion or, even worse, based only on the constituents that were used to grow it.

As represented in Figure 8, when the [PAH−PPCs]$_5$ is dehydrated, it collapses and loses the structure it had acquired via the use of Lyz as a templating agent. The idea that [PAH−PPCs]$_5$ could collapse and lose its structure is consistent with a model in which the latter is highly hydrated after construction. After that, it collapses in the low-RH environment, [PAH−PPCs]$_5$ multilayers share common features with the LbL that

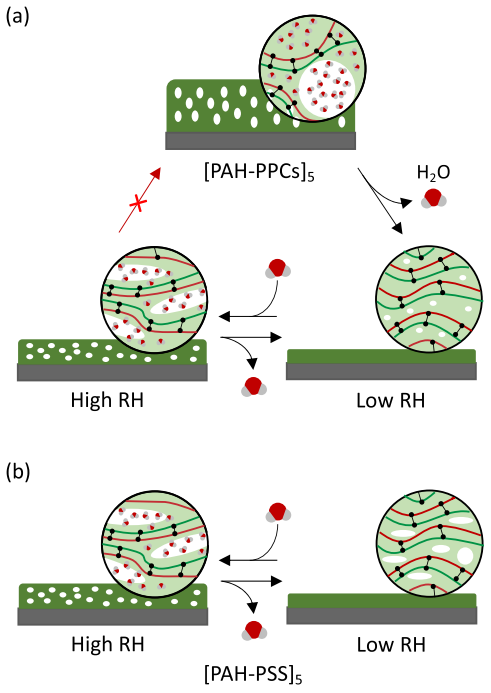

Figure 8. Schematic of the hypothetical structure of (a) [PAH−PPCs]$_5$ and (b) [PAH−PSS]$_5$ systems before and after dehydration. The use of Lyz as a templating element leads to PEMs that are highly hydrated. When dehydrated, these PEMs irreversibly lose water.

https://dx.doi.org/10.1021/acsapm.0c00243
ACS Appl. Polym. Mater. 2020, 2, 2602−2611

has been constructed by directly assembling PAH with PSS, i.e., the water sorption/desorption becomes reversible, and the PE phase separates from the water phase. Nevertheless, the kinetics of the water sorption/desorption differs between both PEMs: a swelling hysteresis is present for $[PAH-PPCs]_5$ but not for $[PAH-PSS]_5$. This result suggests that different water transport mechanisms and polymer chain mobilities are at play in the two PEMs. These can originate either from the different structures of the PEMs or the presence of trace amount of Lyz in the $[PAH-PPCs]_5$. The fitting of the swelling with the Flory–Huggins equation shows that both PEM phases separate when they swell. A different porosity in the two PEMs could thus explain the hysteresis that is observed. Given that $[PAH-PPCs]_5$ shows a swelling hysteresis, it could be argued that the porosity is low and that the water molecules diffuse slowly in the $[PAH-PPCs]_5$ PEM. On the contrary, $[PAH-PSS]_5$ could be more porous which favors water diffusion. This is illustrated in Figure 8.

CONCLUSION

In this paper, $[PAH-PPCs]_5$ and $[PAH-PSS]_5$ PEMs were constructed. These are similar in composition, i.e., mainly made of water, PAH, and PSS, but display drastically different hydration states after their construction. In particular, $[PAH-PPCs]_5$ resembles more a nanogel given its high water content. The latter feature is attributed to the presence of Lyz in PPCs, which is used as a templating agent upon PEM formation. Then, using QCM-D mounted with a humidity module, we show that when $[PAH-PPCs]_5$ is dehydrated, it collapses into a denser PEM and irreversibly loses part of its water content. After its dehydration, $[PAH-PPCs]_5$ has a composition that is similar to $[PAH-PSS]_5$, and further rehydration causes a phase separation between the PE and water, as indicated by fitting the Flory–Huggins equation to the data. However, the dynamics of the swelling/deswelling is not the same in both PEMs. Indeed, a swelling hysteresis was measured for $[PAH-PPCs]_5$ while $[PAH-PSS]_5$ swell and deswell at the same rate. This is due to a different PEM porosity and/or the presence of a trace amount of Lyz. These results show that the use of a templating element in interfacial self-assemblies allows the construction of nanosystems featuring particular architectures (highly hydrated nanofilm) and functionalities (irreversible dehydration and hysteresis upon swelling/deswelling) that cannot be reached when assembly is performed according to a more classical pathway. It thus provides a way to tune the hydration state of LbL assemblies while potentially changing their response to vapor pressure, which is topical for both biomedical and sensing applications.

ASSOCIATED CONTENT

Supporting Information

The Supporting Information is available free of charge at https://pubs.acs.org/doi/10.1021/acsapm.0c00243.

Additional characterization data and experimental details (PDF)

AUTHOR INFORMATION

Corresponding Authors

Christine Dupont-Gillain − *Institute of Condensed Matter and Nanosciences, Université catholique de Louvain, B-1348 Louvain-la-Neuve, Belgium;* orcid.org/0000-0002-6153-4044; Email: christine.dupont@uclouvain.be

Aurélien vander Straeten − *Institute of Condensed Matter and Nanosciences, Université catholique de Louvain, B-1348 Louvain-la-Neuve, Belgium;* orcid.org/0000-0002-5435-1987; Email: aurelien.vanderstaeten@uclouvain.be

Complete contact information is available at: https://pubs.acs.org/10.1021/acsapm.0c00243

Author Contributions

A.v.S. performed the experimental work and result analysis. C.D.-G. supervised the research. The experiments were designed and the manuscript was written through contributions of both authors.

Notes

The authors declare no competing financial interest.

ACKNOWLEDGMENTS

The work was supported by BELSPO, the Belgian Science Policy, through the Interuniversity Attraction Pole Program (P07/05), by the Belgian National Foundation for Scientific Research (FNRS), and by the Research Foundation for Industry and Agriculture (FRIA). The authors thank Thomas Gillis and Adrien Scheuer for their help with the Flory–Huggins equation fitting.

REFERENCES

(1) Zhao, S.; Caruso, F.; Dahne, L.; Decher, G.; De Geest, B. G.; Fan, J.; Feliu, N.; Gogotsi, Y.; Hammond, P. T.; Hersam, M. C.; Khademhosseini, A.; Kotov, N.; Leporatti, S.; Li, Y.; Lisdat, F.; Liz-Marzan, L. M.; Moya, S.; Mulvaney, P.; Rogach, A. L.; Roy, S.; Shchukin, D. G.; Skirtach, A. G.; Stevens, M. M.; Sukhorukov, G. B.; Weiss, P. S.; Yue, Z.; Zhu, D.; Parak, W. J. The Future of Layer-by-Layer Assembly: A Tribute to ACS Nano Associate Editor Helmuth Mohwald. *ACS Nano* **2019**, *13* (6), 6151−6169.

(2) vander Straeten, A.; Lefevre, D.; Demoustier-Champagne, S.; Dupont-Gillain, C. Protein-Based Polyelectrolyte Multilayers. *Adv. Colloid Interface Sci.* **2020**, *280*, 102161.

(3) Mattia, E.; Otto, S. Supramolecular Systems Chemistry. *Nat. Nanotechnol.* **2015**, *10* (2), 111−119.

(4) Secrist, K. E.; Nolte, A. J. Humidity Swelling/Deswelling Hysteresis in a Polyelectrolyte Multilayer Film. *Macromolecules* **2011**, *44* (8), 2859−2865.

(5) Li, D.; Jiang, Y.; Li, Y.; Yang, X.; Lu, L.; Wang, X. Fabrication of a Prototype Humidity-Sensitive Capacitor via Layer-by-Layer Self-Assembling Technique. *Mater. Sci. Eng., C* **2000**, *11* (2), 117−119.

(6) Peyratout, C. S.; Dähne, L. Tailor-Made Polyelectrolyte Microcapsules: From Multilayers to Smart Containers. *Angew. Chem., Int. Ed.* **2004**, *43* (29), 3762−3783.

(7) Rodahl, M.; Höök, F.; Krozer, A.; Brzezinski, P.; Kasemo, B. Quartz Crystal Microbalance Setup for Frequency and Q-Factor Measurements in Gaseous and Liquid Environments. *Rev. Sci. Instrum.* **1995**, *66* (7), 3924−3930.

(8) v. Klitzing, R. Internal Structure of Polyelectrolyte Multilayer Assemblies. *Phys. Chem. Chem. Phys.* **2006**, *8* (43), 5012−5033.

(9) Lösche, M.; Schmitt, J.; Decher, G.; Bouwman, W. G.; Kjaer, K. Detailed Structure of Molecularly Thin Polyelectrolyte Multilayer Films on Solid Substrates as Revealed by Neutron Reflectometry. *Macromolecules* **1998**, *31* (25), 8893−8906.

(10) Farhat, T.; Yassin, G.; Dubas, S. T.; Schlenoff, J. B. Water and Ion Pairing in Polyelectrolyte Multilayers. *Langmuir* **1999**, *15* (20), 6621−6623.

(11) Kügler, R.; Schmitt, J.; Knoll, W. The Swelling Behavior of Polyelectrolyte Multilayers in Air of Different Relative Humidity and in Water. *Macromol. Chem. Phys.* **2002**, *203* (2), 413−419.

(12) Wong, J. E.; Rehfeldt, F.; Hänni, P.; Tanaka, M.; Klitzing, R. V. Swelling Behavior of Polyelectrolyte Multilayers in Saturated Water Vapor. *Macromolecules* **2004**, *37* (19), 7285−7289.

(13) Köhler, R.; Dönch, I.; Ott, P.; Laschewsky, A.; Fery, A.; Krastev, R. Neutron Reflectometry Study of Swelling of Polyelectrolyte Multilayers in Water Vapors: Influence of Charge Density of the Polycation. *Langmuir* **2009**, *25* (19), 11576−11585.
(14) Nolte, A. J.; Cohen, R. E.; Rubner, M. F. A Two-Plate Buckling Technique for Thin Film Modulus Measurements: Applications to Poly Electrolyte Multilayers. *Macromolecules* **2006**, *39* (14), 4841−4847.
(15) Nolte, A. J.; Treat, N. D.; Cohen, R. E.; Rubner, M. F. Effect of Relative Humidity on the Young's Modulus of Polyelectrolyte Multilayer Films and Related Nonionic Polymers. *Macromolecules* **2008**, *41* (15), 5793−5798.
(16) vander Straeten, A.; Bratek-Skicki, A.; Jonas, A. M.; Fustin, C. A.; Dupont-Gillain, C. Integrating Proteins in Layer-by-Layer Assemblies Independently of Their Electrical Charge. *ACS Nano* **2018**, *12* (8), 8372−8381.
(17) vander Straeten, A.; Bratek-Skicki, A.; Germain, L.; D'Haese, C.; Eloy, P.; Fustin, C.-A. A.; Dupont-Gillain, C. Protein−Polyelectrolyte Complexes to Improve the Biological Activity of Proteins in Layer-by-Layer Assemblies. *Nanoscale* **2017**, *9* (44), 17186−17192.
(18) Lehr, B.; Seufert, M.; Wenz, G.; Decher, G. Fabrication of Poly(p-Phenylene Vinylene) (PPV) Nanoheterocomposite Films via Layer-by-Layer Adsorption. *Supramol. Sci.* **1995**, *2* (3−4), 199−207.
(19) Graf, G.; Kocherbitov, V. Determination of Sorption Isotherm and Rheological Properties of Lysozyme Using a High-Resolution Humidity Scanning QCM-D Technique. *J. Phys. Chem. B* **2013**, *117* (34), 10017−10026.
(20) Reviakine, I.; Johannsmann, D.; Richter, R. P. Hearing What You Cannot See and Visualizing What You Hear: Interpreting Quartz Crystal Microbalance Data from Solvated Interfaces. *Anal. Chem.* **2011**, *83* (23), 8838−8848.
(21) Robinson, R. A. The Water Activities of Lithium Chloride Solutions up to High Concentrations at 25°. *Trans. Faraday Soc.* **1945**, *41* (0), 756−758.
(22) vander Straeten, A.; Dupont-Gillain, C. Self-Reorganizing Multilayer to Release Free Proteins from Self-Assemblies. *Langmuir* **2020**, *36* (4), 972−978.
(23) Shultz, A. R.; Flory, P. J. Phase Equilibria in Polymer-Solvent Systems. II. Thermodynamic Interaction Parameters from Critical Miscibility Data. *J. Am. Chem. Soc.* **1953**, *75* (16), 3888−3892.
(24) Mikos, A. G.; Peppas, N. A. Flory Interaction Parameter χ for Hydrophilic Copolymers with Water. *Biomaterials* **1988**, *9* (5), 419−423.
(25) Fu, J.; Fares, H. M.; Schlenoff, J. B. Ion-Pairing Strength in Polyelectrolyte Complexes. *Macromolecules* **2017**, *50* (3), 1066−1074.
(26) Chacko, R. T.; Ventura, J.; Zhuang, J.; Thayumanavan, S. Polymer Nanogels: A Versatile Nanoscopic Drug Delivery Platform. *Adv. Drug Delivery Rev.* **2012**, *64* (9), 836−851.
(27) Picart, C.; Caruso, F.; Voegel, J. C. *Layer-by-Layer Films for Biomedical Applications*; Wiley-VCH Verlag GmbH & Co. KGaA: Weinheim, 2015.
(28) Ghostine, R. A.; Markarian, M. Z.; Schlenoff, J. B. Asymmetric Growth in Polyelectrolyte Multilayers. *J. Am. Chem. Soc.* **2013**, *135* (20), 7636−7646.

https://dx.doi.org/10.1021/acsapm.0c00243
ACS Appl. Polym. Mater. 2020, 2, 2602−2611